Journal of Cleaner Production 275 (2020) 122778

Contents lists available at ScienceDirect

Journal of Cleaner Production

journal homepage: www.elsevier.com/locate/jclepro

Regional variation in climate impact of grass-based biogas production: A Swedish case study

Johan Nilsson [a, *], Cecilia Sundberg [a, b], Pernilla Tidåker [a], Per-Anders Hansson [a]

[a] Department of Energy and Technology, Swedish University of Agricultural Sciences (SLU), SE-750 07, Uppsala, Sweden
[b] Division of Industrial Ecology, Department of Sustainable Development, Environmental Science and Engineering, KTH Royal Institute of Technology, SE-100 44, Stockholm, Sweden

ARTICLE INFO

Article history:
Received 16 December 2019
Received in revised form
12 May 2020
Accepted 10 June 2020
Available online 15 July 2020

Handling editor. M.T. Moreira

Keywords:
Grass cultivation
Biomethane
Soil carbon sequestration
DNDC
Regional-LCA
Soil N_2O emissions

ABSTRACT

Transitioning from a fossil economy to a bio-economy will inevitably increase the demand for biomass production. One strategy to meet the demand is to re-cultivate set-aside arable land. This study investigated the climate impact and energy potential of grass-based biogas produced using fallow land in Uppsala municipality, Sweden. The assessment was performed on regional level for more than 1000 individual sites, using the agro-ecosystem model DeNitrification DeComposition (DNDC) in combination with time-dynamic life cycle assessment methodology. The results showed that the system could significantly increase biogas production within the region, which would reduce the climate impact by 9950 Mg CO_2-eq per year. Compared with diesel fuel, the grass-based biogas gave a GWP reduction of 85%. However, the site-specific GWP reduction showed large spatial variability, ranging between 102 and 79% compared with diesel fuel, depending on where in the region the grass was cultivated. Two alternative scenarios were investigated, increased mineral N fertilisation and inclusion of N-fixing crops in the feedstock mixture. The highest mitigation per biogas energy produced was found for the N-fixing scenario but, because of lower yields, this scenario had lower total mitigation potential for the region than the increased fertilisation scenario. The increased fertilisation scenario had a lower climate mitigation effect per biogas energy produced, but the highest mitigation potential when the whole region was considered, because of the increased biogas production. The method applied in this study can guide land-use planning of local energy production from arable land, also for other regions.

1. Introduction

To avert the most critical harms of global warming, the world must promptly reduce greenhouse gas (GHG) emissions overall and, in particular, from fossil sources (IPCC, 2014). One strategy to phase out fossil sources is to replace them with bio-based alternatives, thus transitioning from a fossil economy to a bio-economy. This transition will inevitably increase the demand for biomass production (Lewandowski, 2015). This increasing demand can partly be met by re-cultivating set-aside arable land, which has low short-term competition with food production and has less impact than conversion of natural land (Tilman et al., 2009). In Sweden, a major challenge in the transition to a fossil-free economy is the transport sector, where about 77% of the energy use is fossil-based (SEA, 2019). The future demand for biofuels is projected to constitute about half the energy use in the sector, both in the intermediate and long-term perspective (SOU, 2013). Biogas is a competitive biofuel option, generated from anaerobic digestion typically of organic wastes, such as food waste and sewage sludge. The produced biogas can replace fossil energy in power and heat generation as well as in transportation. Furthermore, biogas is a storable energy carrier that can be saved for future energy use (Weiland, 2010), and may therefore fit well into energy systems with large shares of renewable intermittent energy sources. In 2017, Swedish production of biogas was 7.6 PJ, of which about two-thirds were upgraded to vehicle fuel, mainly used as fuel for cars and buses. In the same year, the total amount of fuel delivered amounted to 333 PJ (SEA, 2019). Besides energy, the digestate produced in the biogas process can be used as organic fertiliser, reducing the demand for mineral fertiliser and adding carbon (C) to the soil.

Soil C sequestration has been advocated as a cost-effective

* Corresponding author.
E-mail address: johan.e.nilsson@slu.se (J. Nilsson).

https://doi.org/10.1016/j.jclepro.2020.122778

strategy with high potential to mitigate global warming. Soil C is more abundant in perennial cropping systems, owing to greater root biomass production, less exposure to soil disturbance and longer growing seasons (Bolinder et al., 2010). Hammar et al. (2017) showed that willow grown on fallow land in Sweden could generate energy and simultaneously remove C from the atmosphere through enhanced soil C sequestration. One of the most common perennial crops in Sweden is grass, which occupies about 40% of the total arable land (SCB, 2018b). Grass is grown worldwide mainly for fodder, but alternative uses such as feedstock for bioenergy purposes are becoming more common (Carlsson et al., 2017).

Life cycle assessment (LCA) is a quantitative method for studying the environmental burden of products and services in a life cycle perspective, from cradle to grave. The method was initially developed as a site and time-independent tool for industrial systems but, over time, has become applicable for other types of systems. For LCAs involving agricultural processes, spatial and temporal dynamics could have a significant impact on the total environmental performance. For example, the GHG balance is heavily dependent on properties such as soil type, climate and agricultural practices (Miller et al., 2006). However, LCA studies that include fine-scale spatial differentiation over time and space are quite rare, due to the large data demand (Nitschelm et al., 2016).

Previous studies have shown that agro-ecosystem models can be used in LCAs to generate site-specific data (Goglio et al., 2018b, 2014). In an earlier study (Nilsson et al., Unpublished results), we combined LCA methodology and the agro-ecosystem model DNDC to assess the environmental impact of grass cultivation at five sites in Sweden. In the present study, we extended the system to grass-based biogas production on regional level, using set-aside arable land in Uppsala municipality, located in east-central Sweden. In Uppsala municipality, about 10% of total arable land is reported to be under fallow (SCB, 2018a), of which more than 50% has been unused for more than three consecutive years (SCB, 2017).

The overall aim of this study was to assess the energy potential and climate impact of converting current unused arable land in Uppsala municipality to intensified grass cultivation and using the harvested biomass to produce biogas. The investigation was performed on a regional level, using existing site-differentiated data. The GHG balance was investigated for each study site, including changes in the soil C stock. The climate impact of the fuel produced (MJ^{-1}) was compared with that of diesel fuel, while accounting for the higher energy efficiency in a diesel engine. Moreover, the climate impact variation within the region was analysed, as was the effect of choosing the most suitable sites.

2. Method and materials

2.1. System boundary

The system boundary included grass cultivation, biogas production, digestate use and biogas use. The grass cultivation was assumed to be located on mineral soils under fallow in Uppsala municipality. The assessment was performed over a 100-year time horizon, which corresponded to 20 grass rotations. Any other co-substrates mixed in the digester were outside the system boundary for this study. Since the land was assumed to be initially unused, no indirect land-use changes were accounted for. The direct land-use effects were defined as the impact of transferring the land from the reference land use (fallow) to the altered land use (grass cultivation) throughout the investigated time horizon. Expansion of infrastructure, such as construction and manufacturing of trucks and machinery and other capital goods were not included in the assessment since their climate impact has been demonstrated to be of minor importance compared to other activities in the system (Hijazi et al., 2016; Tidåker et al., 2016a). All major fluxes of the three main GHGs (CO_2, CH_4 and N_2O) were included in the climate impact assessment. The system was analysed in terms of three different units: (i) hectares (ha) of land, (ii) all investigated fields in Uppsala municipality and (iii) biogas energy produced (MJ). The ha-based unit was used in the inventory analysis to show the effect of land-use change, the field-based unit was used to show the climate impact of increased biogas production in the municipality using fallow land for biogas production, and the biogas-based unit was included to provide figures comparable with results from other bioenergy studies.

2.2. Study region

The study region, Uppsala municipality, is located in east-central Sweden. Information about current land use was obtained from the Swedish Board of Agriculture. The reported fallow land in the region in 2014 was 1977 sites, with a total area of 3587 ha. Organic soils (soil organic matter (SOM) > 20%) and sites smaller in area than 0.5 ha were omitted from the study, which reduced the number of sites to 1240, with a total area of 3006 ha. Fine-textured soils such as silty clay loam, clay loam, silty clay and clay together constituted about 90% of the total area assessed, while more coarse-textured soils were less frequent. The soil C content showed considerable variation, ranging between 0.7 and 11.5%, with a median value of 2.2%. The distribution of soil texture and C content is shown in Fig. S1 in Supplementary Material. The soil pH value ranged from 5.1 to 8.3, with a median value of 6.5. The weather data used consisted of a 10-year sequence, collected between 2007 and 2016, which was repeated in the model within the temporal boundary of the system studied. Mean annual precipitation for this period was 596 ± 77 mm, and mean annual temperature was 6.5 ± 0.9 °C. We assumed the same location for the biogas plant as for the current largest existing plant in the region (Fig. 1).

2.3. System description

The studied system was divided into six subsystems: grass cultivation (*GrassC*^{A}), biomass conversion (*BioC*^{A}), digestate (*Dig*^{A}), fallow (*Fall*^{R}), fossil fuel (*Foss*^{R}) and mineral fertiliser (*Min*^{R}) (Fig. 2).

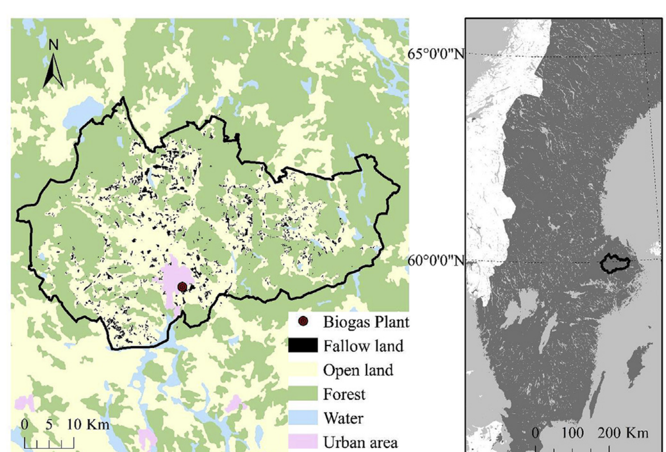

Fig. 1. (Left) Map of the study region, Uppsala municipality (inside the black line), showing the distribution of fallow land (black dots) and the location of the biogas plant (red and blackpurple dot). (Right) Location of the region in east-central Sweden. (For interpretation of the references to colour in this figure legend, the reader is referred to the Web version of this article.)

The first three subsystems comprised the altered system (A) and the latter three the reference system (R). The subsystems were also clustered into three compartments, land use (ΔLU), fuel production (ΔFP) and soil fertilisation (ΔSF), to assess the net impact of the different steps in the life cycle. The emissions (*E*) from ΔLU were assessed as the difference between $GrassC^A$ and $Fall^R$, those from ΔFP as the difference between $BioC^A$ and $Foss^R$ and those from ΔSF as the difference between Dig^A and Min^R. The basis of the comparison in the ΔLU compartment was area, i.e. the calculated emissions were based on the same area of grass cultivation and fallow. For the ΔFP compartment, engine energy was the basis for comparison, while for the ΔSF compartment it was nitrogen (N) uptake. The total GHG emissions (E_{Tot}) were calculated as the difference between the altered system and the reference system as:

$$E_{Tot} = \overbrace{\left(E_{GrassC^A} - E_{Fall^R}\right)}^{E_{\Delta LU}} + \overbrace{\left(E_{BioC^A} - E_{Foss^R}\right)}^{E_{\Delta FP}} + \overbrace{\left(E_{Dig^A} - E_{Min^R}\right)}^{E_{\Delta SF}} \quad (1)$$

2.3.1. Land use

The net climate impact from ΔLU was assessed by subtracting the impact of $GrassC^A$ from the impact of the $Fall^R$ subsystem (Fig. 2).

In $GrassC^{A,}$ the grass, a mixture of timothy (*Phleum pratense* L.) and meadow fescue (*Festuca pratensis* Huds.), was grown in five-year consecutive rotation periods. The rotation started with sowing and rolling in the first year and ended with ploughing. During the rotation period, the grass was cut, chopped and fertilised with mineral fertiliser twice a year. In total, 140 kg N fertiliser were applied per ha and year. At each cut, 85% of the aboveground biomass was assumed to be harvested.

Diesel consumption for sowing, rolling and spreading fertiliser was set to 2.3, 2.3 and 4.7 dm^3 ha^{-1}, respectively, whereas diesel consumption for cutting, chopping and ploughing was based on linear regression models with biomass yield and clay content as the independent variable (Eq. S1). The GHG emissions from mineral fertiliser manufacturing were 3.6 kg CO_2-eq kg N^{-1}, where the climate impact was set to 86% from CO_2 emissions, with the remaining 14% from N_2O (Brentrup et al., 2016).

The fallow land was assumed to be covered with vegetation, so-called green fallow. The only field operation conducted on the fallow land was cutting, which was performed once a year during late autumn. The cut biomass was left in the field.

2.3.2. Fuel production

The net climate impact from ΔFP was calculated as the difference between $BioC^A$ and $Foss^R$ (Fig. 2). After each cut, the harvested feedstock was transported to the biogas plant with freight trucks. The energy consumption for using a truck with trailer, load capacity 34–40 Mg, was taken from https://www.transportmeasures.org. The energy use per transport Mg x km was 1 MJ, including empty positioning of the truck.

At the biogas plant, the harvested biomass was loaded into bunker silos. The diesel consumption for biomass compaction in the silo was calculated based on the weight of the compressed biomass (Eq. S2). Biogas energy produced was derived based on the amount of biomass added to the biogas reactor and the specific CH_4 production, 280 Nm^3 Mg VS^{-1}, where the volatile solids (VS) content was set to 92% of dry matter (DM). The ensiled biomass was continuously fed to the biogas reactor, where mesophilic anaerobic digestion converted the biomass to biogas that was upgraded to bio-methane. A part of the biogas produced was used to heat the reactor. The biogas conversion processes pumping, stirring, upgrading and gas compression were all considered to be electrically driven. Emissions and primary energy use for the electricity were assessed using data for the Nordic electricity mix, which was assumed to be close to the expansion margin based on the stated goal of a continuous high share of renewables in the Swedish electricity mix (Government Offices of Sweden, 2016). After the digestion, the digestate produced was assumed to be stored, before being transported to farms and spread in winter wheat cultivation.

The CH_4 losses from biomass conversion were assessed using data from the existing plant in Uppsala for 2015, when measured losses during anaerobic digestion and upgrading with water scrubbers were 0.01% and 0.3% of methane production, respectively (Uppsala Vatten, 2017). The losses from digestate storage were calculated using the equation for large and medium-sized biogas plants given by Styles et al. (2016) (Eq. S2).

The biogas produced was assumed to replace diesel fuel, $Foss^R$. In the calculations, the higher efficiency in the diesel engine was considered by using an energy efficiency of 9.8 MJ km^{-1} for the diesel compared with 11.4 MJ km^{-1} for the biogas (Börjesson et al., 2016). Hence, one MJ biogas replaced 0.86 MJ of diesel.

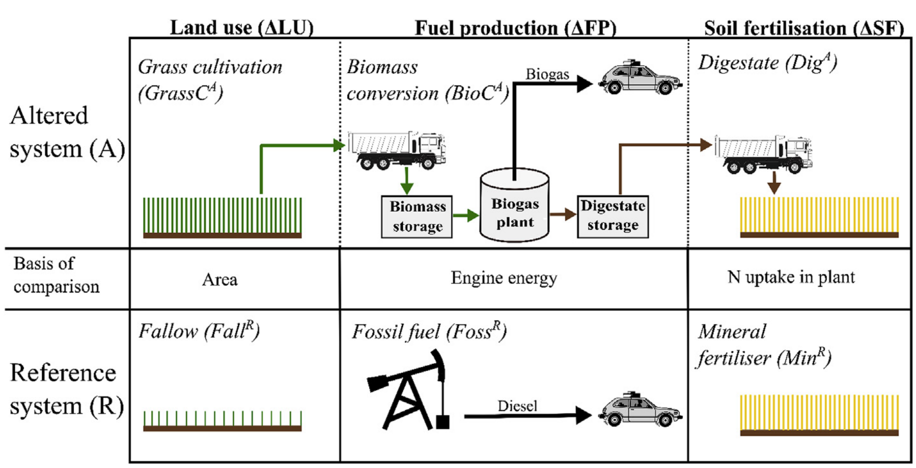

Fig. 2. Schematic illustration of the grass-based biogas system studied, divided into six subsystems: Grass cultivation ($GrassC^A$), Biomass conversion ($BioC^A$), Digestate use (Dig^A), Fallow ($Fall^R$), Fossil fuel ($Foss^R$) and Mineral fertiliser (Min^R). The net effect of the system was calculated as the difference between altered system and reference system. The subsystems were also divided into three compartments: Land use ($GrassC^A$ - $Fall^R$), Fuel production ($BioC^A$ - $Foss^R$) and Soil fertiliser (Dig^A - MinR). The basis of comparison is shown in the row between the altered system and the reference system.

2.3.3. Soil fertilisation

The net effect of the ΔSF compartment was calculated by subtracting the GHG emissions occurring in winter wheat cultivation with mineral fertiliser (Min^R) from the emissions from winter wheat cultivation with digestate fertiliser (Dig^A) (Fig. 2).

The digestate was transported once a year to the winter wheat sites. The distance to the winter wheat cultivation was set to 20 km based on the mean distance to the fallow land from the biogas plant. At pick up, the DM content was 9.5% for the digestate. All transport was performed with the same type of truck as in $BioC^A$.

For the cultivation with mineral fertiliser, the amount of N applied was 135 kg ha^{-1}. The same spreading technique was used as for the grass cultivation subsystem. The amount of digestate produced in the system was calculated by following the mass balance from biomass input to the reactor to field application (Fig. 3).

The C and N content of the digestate was obtained by calculating the C losses in the form of CO_2 and CH_4 conversion during anaerobic digestion and CH_4 emissions during the digestate storage phase. The biogas before upgrading was assumed to contain 55% CH_4. The N content in the digestate at application was assessed by calculating the losses of N, in the form of N_2O and NH_3, during digestate storage (Fig. 3). The equation used to calculate the conversions is presented in Supplementary Material (Eq. S3).

In order to compare the digestate to the mineral fertiliser, the mineral fertiliser equivalent (MFS) was calculated to represent the difference in fertilisation effect, i.e. how much digestate was needed to replace the mineral N, given the specific composition of the digestate. The MFS was obtained by iteratively executing the agro-ecosystem model (section 2.4.2) with different amounts of applied digestate until the average yields corresponded. The MFS for the digestate produced was found to be 80%, leading to a total amount of digestate spread per hectare of 37.1 Mg (wet weight), containing 1183 kg C and 169 kg N (tot-N). The digestate properties are presented in Table S1. The diesel consumption for spreading the digestate was 0.31 dm^3 MJ^{-1}.

2.4. Life cycle inventory analysis

2.4.1. GIS model

The ArcGIS product (ArcMap version 10.3, ESRI, Redlands, CA, USA) was used to link soil data to the specific study sites in the region. All land reported as being under fallow was linked to specific soil properties, in terms of initial soil organic matter, clay, silt and sand content and pH. This was done by interpolating data from 258 measurement points spread out over the study region. ArcGIS was also used to calculate road route distances from the grass cultivation sites to the biogas plant.

2.4.2. Agro-ecosystem modelling

The process-based agro-ecosystem model DNDC (DeNitrification DeComposition) was first developed in 1992 to model C and N fluxes in agricultural soils (Li et al., 1992). Since then, the model has been updated and branched into several versions, which have been used in studies all over the world (Gilhespy et al., 2014). In the present study we used the Canadian version, DNDC-CAN, which has been validated in similar cool-weather conditions as those prevailing in Sweden. Following an assessment of different methods for estimating soil-borne N_2O and CO_2 emissions, Goglio et al. (2018a) concluded that DNDC was the only model among those tested that gave similar results to measurements for N_2O emissions estimates. Here, the model was used to generate annual, site-specific, inventory data comprising biomass yields, soil C balances and soil N_2O and CH_4 emissions. The input variables field capacity, wilting point porosity and bulk density were estimated using a pedotransfer model developed by Saxton and Rawls (2006).

The crop and management model set-up was the same as in Nilsson et al. (Unpublished results), in which the same grass mixture was modelled at five locations in Sweden. The fallow land was simulated with the same set-up as for the grass crop, but without added fertiliser. In order to capture the initial effect of the grass-based biogas system, the simulation was formulated to include a spin-up period with the reference system land use, which was executed before collection of the inventory data started. We used a spin-up period of 10 years, which is typically used for the DNDC model (Grant et al., 2016).

The effect of using the digestate as fertiliser was analysed by executing the DNDC model for winter wheat cultivation, both with digestate application and mineral fertiliser. In contrast to the $GrassC^A$ subsystem, which was modelled for all 1240 fields, Dig^A was modelled for one field which represented the average conditions in the region. Both fertiliser options were assessed with the same management procedure, in terms of timing for ploughing, harvesting and spreading fertiliser. The winter wheat area for which the N demand could be met by the digestate produced from 1 ha of grass cultivation, here denoted F_{dig}, was calculated as:

$$F_{dig} = \left(N_{dig} - N_{NH3\ loss\ app}\right) \Big/ N_{demand} \tag{2}$$

F_{dig} was multiplied by the GHG emissions per hectare for the simulated winter wheat cultivation to obtain the GHG balance from the *Dig* subsystem, where N_{dig} (kg N ha^{-1}) is the N in the digestate, $N_{NH3\ loss\ app}$ (kg N ha^{-1}) is the N–NH_3 losses during digestate application, and N_{demand} (kg N ha^{-1}) is the N demand of winter wheat, i.e. the amount of mineral N applied divided by MFS (explained in section 2.3.3). Model input parameters for all the different land uses are listed in Table S2.

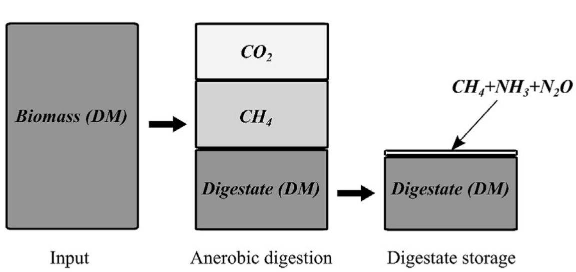

Fig. 3. Conceptual model of the mass balance calculation for digestate (illustration not to scale).

2.4.3. Energy conversion

The energy output from the altered system was calculated at regional level. The major primary energy input, in terms of fossil fuel and electricity, was included. The biogas produced was assumed to be partly used to heat the biogas plant, so heat was not considered an energy input. The energy performance of the altered system was finally assessed by calculating the energy ratio (ER) (Djomo et al., 2011), calculated as the ratio of energy produced to primary energy input:

$$Energy\ ratio = Energy\ output / Primary\ energy\ input \tag{3}$$

2.5. Climate impact assessment

The climate impact was assessed both with GWP methodology and with Absolute Global Temperature Potential (AGTP), defined by Myhre et al. (2013). The latter approach is used to assess the temperature response, in Kelvin (K), to changes in radiative forcing caused by GHG fluxes. All GHGs have different impacts on radiative forcing, depending on atmospheric lifetime and radiative efficiency, i.e. the impact on the balance of incoming solar and outgoing terrestrial radiation. The annual net fluxes of all major GHGs (CO_2, CH_4 and N_2O) from the system were annually aggregated and converted to temperature response over the analytical time horizon, 100 years. This rather extensive time frame was adopted to enable investigation of the time dynamic variation of the climate impact of the system. The temperature response for each year was then accumulated for each of the simulated years as:

$$\Delta T_i(H) = \sum_{t=0}^{H} X_i(t) AGTP_i(H - t) \tag{4}$$

where $\Delta T_i(H)$ is the cumulative temperature response to the flux of GHG i during analytical time horizon H, $X_i(t)$ is the total flux of GHG i in year t, and $AGTP_i(H - t)$ is the temperature response of GHG i flux between the time t and the analytical time horizon H per unit GHG. This approach can be used to assess the dynamic climate impact and has previously been used in LCA studies to evaluate the climate impact of bioenergy systems (e.g. Hammar et al., 2017).

A more common approach to assess the climate impact is determination of Global Warming Potential (GWP), where the radiative forcing caused by a pulse emission of a GHG is calculated and compared with the same amount of CO_2 over a specific time horizon, normally 100 years. In contrast to the dynamic AGTP approach, GWP does not include the timing of the GHG flux, which means that emissions that occur during different points in the life cycle are added together, although the endpoint of the impact differs (Kendall, 2012). The characterisation factors used here in GWP calculations were 34 and 298 for CH_4 and N_2O, respectively, with the inclusion of climate-carbon feedbacks (Myhre et al., 2013). The net GWP for the biogas produced, without fossil fuel substitution, was compared to diesel by calculating the GWP reduction from replacing the fossil alternative with the biogas:

$$GWP\ reduction = (GWP_F - GWP_B) / GWP_F \tag{5}$$

where GWP_B is the GWP caused by net emissions from the system under study, without fossil fuel substitution (i.e. $E_{Tot} - E_{Foss^R}$), and GWP_F is the GWP caused by emissions from an equivalent amount of fossil fuel (E_{Foss^R}).

PE input (TJ y^{-1})	
Grass cultivation (*GrassC^A*)	
Ploughing	0.5
Sowing	0.1
Rolling	0.1
Cutting	0.8
Chopping	2.8
Fertiliser manufacturing	14.8
Fertiliser spreading	1.1
Biomass conversion (*BioC^A*)	
Grass transport	1.2
Compaction	1.3
Pumping stirring	5.5
Upgrading	9.1
Compression	7.9
Digestate use (*Dig^A*)	
Transport digestate	1.7
Application	0.9
Total PE input	*47.8*
Energy output (TJ y^{-1})	
Biogas (fuel)	167.4
Total energy output	*167.4*
Energy ratio (GJ GJ^{-1})	3.5

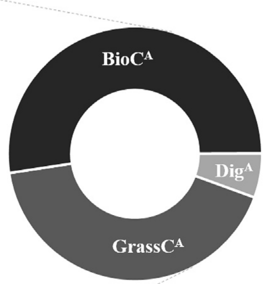

Fig. 4. Annual primary energy (PE) input and energy output of the altered system for the study region, divided between the subsystems grass cultivation (GrassC^A), biomass conversion (BioC^A) and digestate use in winter wheat cultivation (Dig^A).

2.6. Alternative scenarios

Two alternative scenarios were compared with the base scenario, the grass-based biogas system described in section 2.3. These were: (i) increased mineral fertilisation rate in the *GrassC^A* subsystem, from 140 to 200 kg N ha^{-1} and (ii) exclusion of all mineral fertiliser in the *GrassC^A* subsystem based on the assumption that the feedstock crop can satisfy its N demand through biological N fixation from the atmosphere, e.g. a grass-clover mixture. Both alternative scenarios were simulated in DNDC, with otherwise the same model set-up. For the N fixation scenario, the fixation rate was adjusted so that the average yield was about 15% lower than for the base scenario (Tidåker et al., 2016b).

3. Results

3.1. Inventory results

3.1.1. Energy balance

The annual primary energy input and energy output from the altered system are shown in Fig. 4. On a yearly average using all 1240 land sites, the vehicle fuel produced amounted to 167 TJ biogas y^{-1}, with a primary energy input of 47.8 TJ. This resulted in an energy ratio of 3.5, which means that for every energy unit input in terms of fossil fuel and electricity, the system produced 3.5 units of biogas fuel. The highest primary energy input was in *BioC^A*, where upgrading and compression were the processes with the highest energy use. For *GrassC^A*, most energy input was required for manufacturing the mineral fertiliser, which represented 31% of the total energy input. The energy gained from replacing mineral fertiliser with digestate was not included in the energy balance.

3.1.2. Soil carbon balance

The modelled soil C balance of *GrassC^A* showed large differences between the different sites (Fig. 5). In the field with the highest ability to sequester C, the stock was increased by 16 Mg C ha^{-1} during the study period, which corresponded to a sequestration rate of 160 kg C ha^{-1} y^{-1} averaged over the simulated 100 years. The C sequestration rate was higher during the first part of the period than in the latter part. This pattern was more evident in the soil with the median change, 6 Mg C ha^{-1}, where the C stock reached equilibrium in the first half of the simulated period. The site with the lowest ability to sequester C lost 13 Mg C ha^{-1}. Large variation between the sites was also seen for the *Fall^R* subsystem (Fig. 5). Compared with the gross effect of *GrassC^A* and *Fall^R*, the net effect of ΔLU showed lower spatial variability, ranging between 10 and 4 Mg C ha^{-1} with a median increase of 6 Mg C ha^{-1}. The net effect indicated an increased soil C stock at all sites, which means that 100 years of grass cultivation resulted in a larger soil C stock in the region than continued fallow land.

The soil C balance was further investigated by simulating the effect of digestate use on soils with median soil properties in the region. The use of digestate in winter wheat cultivation increased the soil C stock while the mineral fertiliser showed depletion, which entailed a large C increasing net effect of the ΔSF of 23 Mg C ha^{-1} (Fig. 6). On average, the mean digestate produced per ha grass cultivation covered the N demand of 0.66 ha of winter wheat cultivation.

The correlations between input data soil properties and the soil C sequestration potential in *GrassC^A* were analysed using Pearson correlation coefficient (r) (Table S3). The strongest correlation was found for initial C content, which had a negative correlation with

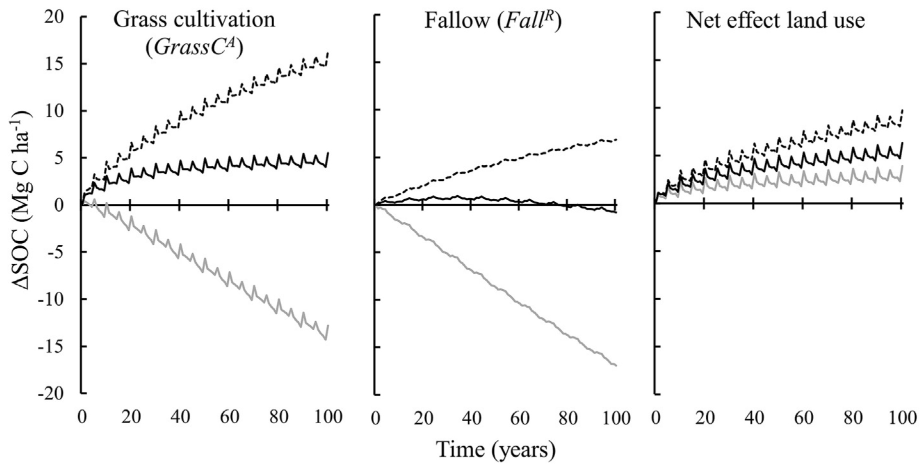

Fig. 5. Cumulative change in soil organic carbon (SOC) over 100 years for all sites investigated (N = 1240), simulated with the DNDC model, for (left) grass cultivation only, (centre) fallow land only and (right) the net effect of changing the land use from fallow to intensified grass cultivation. The dashed black line represents the 95th percentile (max), the grey line the 5th percentile (min) and the black line the median.

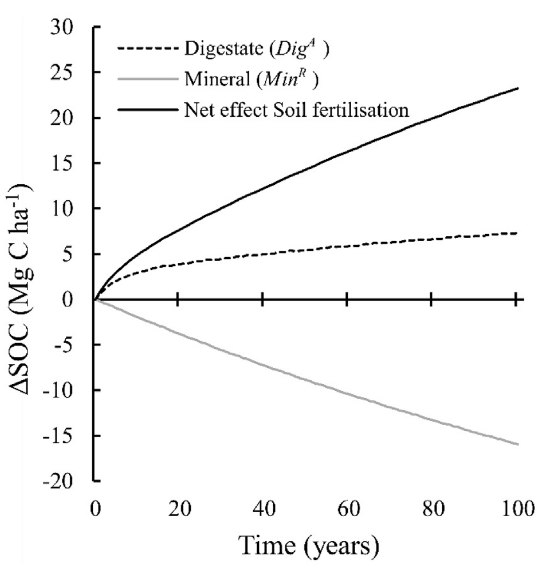

Fig. 6. Cumulative change in soil organic carbon (SOC) over 100 years, simulated with DNDC model, for winter wheat cultivation with biogas digestate as fertiliser (dashed), mineral fertiliser (grey) and the net effect, i.e. the difference between digestate and mineral fertiliser (black). The DNDC model was executed with the input parameters setup that represented the average conditions in the region.

cumulative change in C content. The second highest correlation was for clay content, which had a positive correlation with cumulative change in C content.

3.1.3. Soil nitrous oxide emissions

The modelled soil N_2O emissions also displayed large variations between different sites and years. In general, N_2O emissions from *GrassC*^{A} were higher than from *Fall*^{R} (Fig. 7). This entailed a mean increased soil N_2O net effect, which ranged between 2.0 and 0.2 kg N_2O ha^{-1} y^{-1}, with 1.3 kg N_2O ha^{-1} y^{-1} from the median soil.

For the ΔSF compartment, the net N_2O emissions were low or negative during the earlier part of the study period and increased over time. The mean net N_2O emissions from the soil fertiliser compartment were 0.50 kg N_2O ha^{-1} y^{-1}, i.e. the digestate application in the winter wheat cultivation increased the emissions of N_2O compared with mineral fertiliser. The soil N_2O emissions in *GrassC*^{A} had the highest correlation with soil pH, which showed a negative relationship. The second most influential parameter was the initial C content, which showed a positive relationship (Table S3).

3.2. Climate impact assessment

The climate impact assessment revealed a net decreased temperature response over the study period (Fig. 8). Although the altered system entailed an increased temperature over the time horizon studied, the impact was far lower than that from the reference system. This was largely attributable to the substitution of diesel fuel. The increased soil C stock in the ΔLU compartment was not large enough to compensate for other emissions in the subsystem, primarily because of the emissions from fertiliser manufacturing and the elevated soil N_2O emissions from fertiliser usage. The net effect from the ΔSF compartment was a negative temperature response due to the net increase in the regional soil C stock together with the substitution of mineral N fertiliser.

For the altered system, the impact was dominated by emissions from the *GrassC*^{A} and the *BioC*^{A} subsystems. In the short-term, the emissions from *BioC*^{A} determined the magnitude of climate impact. However, over time, the impact of the *GrassC*^{A} became increasingly significant. This was because the principal GHG emitted from biomass conversion was CH_4, through losses during biogas processing and digestate storage, where about 60% of the CH_4 emissions were from losses during digestate storage. Methane is a relatively short-lived climate forcer, which explains the declining climate impact rate over time (Fig. 8).

For all sites in the region, the net GWP of the biogas produced without fossil fuel substitution (*Foss*^{R}) was 10 g CO_2-eq MJ^{-1}, which corresponded to a GWP reduction of 85% compared with diesel fuel. When only the best-performing sites from a climate change perspective were selected, the GWP reduction compared with the fossil alternative increased. The total GWP reduction in relation to the fraction of study region land used in the biogas system is shown in Fig. 9. For instance, if only 10% of the best-performing sites were included, the GWP reduction increased to 95%.

The spatial difference in the GWP reduction was further investigated (Fig. 10). The impact varied between −1 and 14 g CO_2-eq MJ^{-1} in the study region, which corresponds to a GWP reduction of 102 to 79% compared with diesel. The variation could at large be explained by differences in net soil N_2O emissions, r = 0.97, which in turn were most affected by soil pH (Table S3). In contrast, net

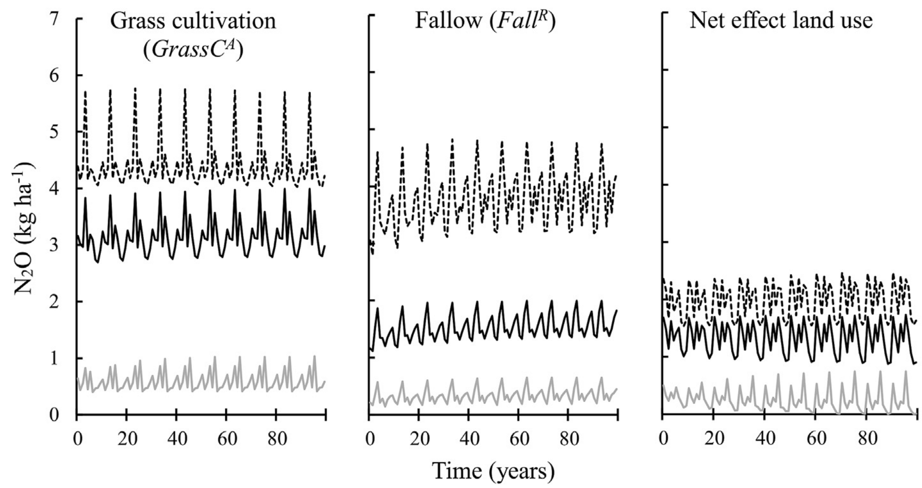

Fig. 7. *Annual soil nitrous oxide (N_2O) emissions for (left) the grass system and (centre) fallow land, and (right) net emissions for feedstock cultivation during 100 years for all sites investigated (N=1240). The dashed black line represents the 95th percentile soil (max), grey line the 5th percentile soil (min) and the black line the median soil.*

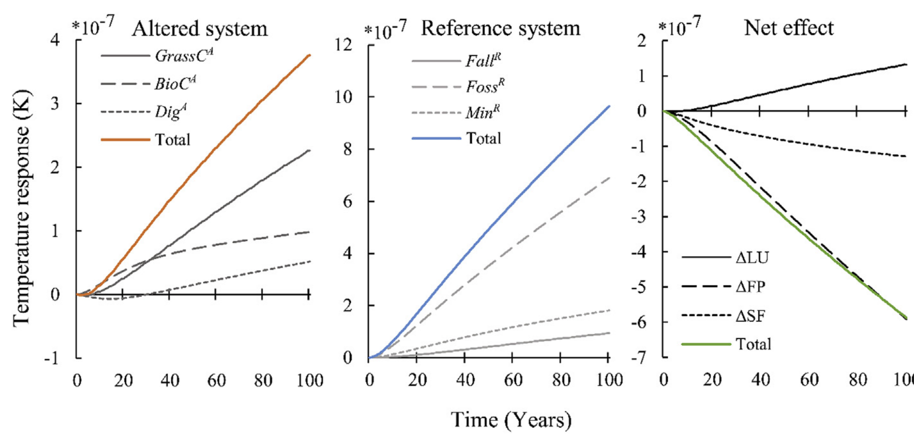

Fig. 8. Temperature response, in degrees Kelvin (K) and using all fields studied (N = 1240, 3006 ha) in the region, for (left) the altered system and (centre) the reference system, and (right) the total net effect.

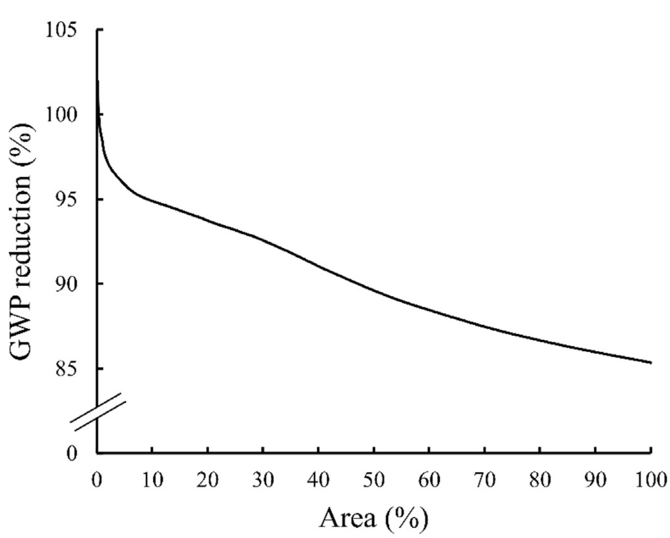

Fig. 9. Global warming potential (GWP) reduction compared with diesel from using the grass-based biogas system, without fossil fuel substitution ($Foss^R$), in relation to fraction of total area used in the region.

changes soil C stock had a low impact on the spatial variation in climate impact (r = −0.28).

3.3. Climate impact of alternative scenarios

The climate impact of the grass-based biogas system and that of the two alternative scenarios (increased fertiliser intensity in $GrassC^A$ and $GrassC^A$ with biological N-fixation) are shown in Fig. 11. The temperature response of the different scenarios was assessed both per biogas energy produced (MJ) and for all fields investigated in Uppsala municipality. The biogas produced in the scenario with increased fertilisation rate showed the lowest climate change mitigation per MJ, -3.4 K$*10^{-17}$, which was similar to that in the base scenario, -3.5 K$*10^{-17}$. The scenario with biological N fixation produced the biogas with the highest mitigation per MJ, -4.6 K$*10^{-17}$. However, due to the assumption of lower yields, this scenario had the lowest overall biogas production, which resulted in lower total mitigation potential for the study region compared with the increased fertilisation scenario. In contrast, the increased fertilisation intensity scenario entailed greater biogas production, which led to the highest climate change mitigation potential for the region. Both alternative scenarios showed greater potential for climate change mitigation in the study region than the base scenario.

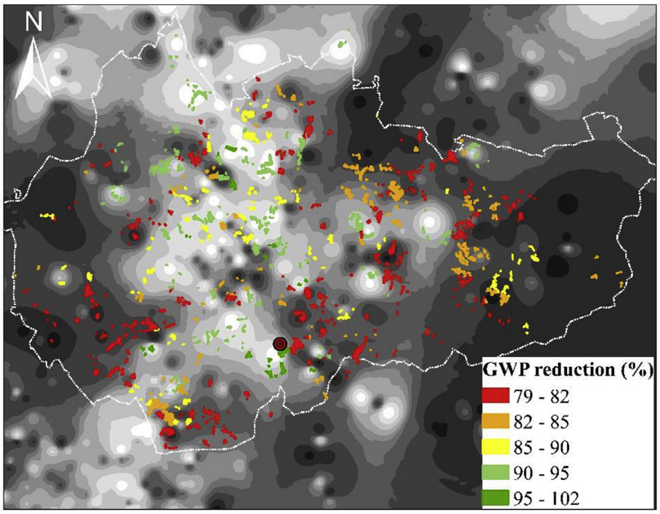

Fig. 10. Spatial variation in global warming potential (GWP) reduction compared with diesel of using the grass-based biogas system, without fossil fuel substitution (Foss[R]). Colours indicate site-specific GWP reduction. Background indicates the soil pH, where a darker shade indicates lower pH. The white dashed line represents the municipality border. (For interpretation of the references to colour in this figure legend, the reader is referred to the Web version of this article.)

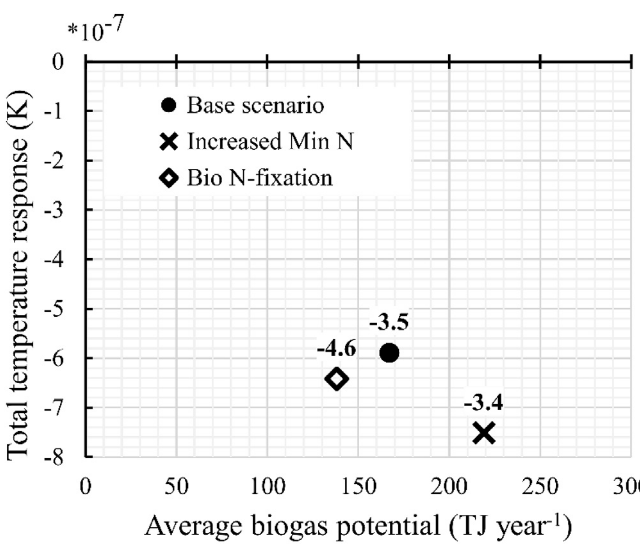

Fig. 11. Total temperature response (degrees K), over 100 years, and average biogas potential (TJ per year) for the base scenario and for two alternative scenarios: increased fertilisation and use of biological N-fixing crops. The numbers next to the icons show the temperature response per unit of biogas produced ($K*10^{-17}MJ^{-1}$).

4. Discussion

In this study, we investigated the energy potential and climate impact of utilising set-aside arable land in Uppsala municipality to produce grass-based biogas. The system studied showed considerable energy potential, with an annual production rate of 167 ± 14 TJ, which would more than double the current biogas production in Uppsala municipality. Besides biogas, the system also produced digestate that could substitute mineral N fertiliser use corresponding to 1980 ha of winter wheat cultivation. The energy ratio for the biogas system was 3.5 (Fig. 4). Energy ratio for large-scale biogas production typically ranges between 2.5 and 5, without including upgrading (Berglund and Börjesson, 2006). Grass-based biogas is usually at the lower end of this range, because of mineral fertilisation and the need for handling the biomass before anaerobic digestion.

The total regional climate impact of the biogas system showed a lower temperature response compared with the reference system (Fig. 8). Based on GWP calculations, biogas from the study system without fossil fuel substitution had a climate impact of 10 g CO_2-eq MJ^{-1} when all 1240 sites with fallow land (3006 ha) were included. This resulted in a GWP reduction of 85% compared with diesel (Figs. 9 and 10). Consequently, using the biogas produced instead of the fossil alternative would considerably decrease the amount of GHG emissions, by about 9950 Mg CO_2-eq y^{-1}.

The biogas system acted as a net atmospheric sink of C, mostly through C sequestration in the ΔLU and the ΔSF compartments. Soil C sequestration is a time-dependent reversible process, where the intrinsic dynamics are a balance between C input and output. For soils that are in equilibrium, i.e. C input equals C output, an increased input will result in an increased soil C stock. The C stock will continue to increase until the soil reaches a new dynamic equilibrium, with the rate of increase normally being faster at the beginning and then levelling off (Kätterer et al., 2012). The temporal aspect is therefore essential when including C balance in a climate impact assessment, as demonstrated by the simulated soil C balance in the present study (Figs. 5 and 6). For instance, the C sequestration rate in grass cultivation with the median soil C change was about five-fold higher in the first 10 years than when averaged over the 100-year study period.

The simulated grass cultivation resulted in a larger gross C stock at most sites investigated (Fig. 5). However, the change in C stock varied between locations. This variation was mainly attributable to initial soil C and clay content, with soils with low initial C stock and high clay content having a greater ability to sequester C. This agrees with findings in previous studies (Bolinder et al., 2010; Poeplau et al., 2015). The simulated C input was quite low on the fallow land, on average 1.7 Mg ha^{-1}. Greater biomass production on this fallow land would reduce the net soil C increase at the sites investigated. Compared with the ΔLU compartment, the net effect of using digestate as fertiliser was a greater net increase in the soil C stock in the ΔSF compartment. This was mainly because of the high C depletion for the winter wheat cultivation with mineral fertiliser. The effects on the soil C balance of using digestate from grass-based biogas production are unfortunately poorly documented. Tatzber et al. (2012) performed long-term field trials of degradation of different organic amendments, e.g. farmyard manure, for which they concluded that the C fraction remaining in the soil after 5, 10 and 37 years was 30%, 20% and 9%, respectively. Using these figures, the soil C sequestration from digestate application would be 10 Mg ha^{-1} over 37 years, which indicates that our estimates may be slightly low.

The simulated soil-N_2O emissions were generally higher for grass cultivation than for fallow land, due to the use of N-fertiliser (Fig. 7). The net N_2O emissions from the ΔLU compartment showed great variation between sites. The strongest correlation to input data was with pH and initial C content (Table S3), indicating that soils with lower pH and high C content generate higher N_2O emissions. Experimental studies have shown that pH affects the ratio between N_2O and N_2 emissions, with increasing N_2O emissions with decreasing pH, which has been attributed to the interference of N_2O denitrification in environments with lower pH (e.g. McMillan et al., 2016; Russenes et al., 2016). Soil N_2O emissions from the ΔLU compartment explained the largest proportion of the net spatial variation in climate impact.

N_2O is a very potent GHG, 298 times stronger than CO_2 over a 100-year perspective. Strategies to increase soil C by intensifying fertilisation may, therefore, be precarious, since soils are not infinite

C sinks. When the soil reaches a new C equilibrium, it will no longer sequester C. However, soil N_2O emissions induced by increased fertilisation rate will continue. Stopping fertilisation at that point would eventually cause lower primary production and hence lower C input, leading to soil C losses. Thus, the effects of increasing the fertilisation rate could go from climate mitigating to climate forcing.

The scenario analysis showed that increasing fertilisation in *GrassC^A* entailed increasing climate change mitigation potential for the study region compared with the base scenario (Fig. 11). This effect was attributed to the increased biogas production, which meant that the system could substitute more diesel fuel. On the other hand, the scenario with biological N fixation displayed the highest climate efficiency, meaning the highest mitigation per biogas energy produced (MJ). The greatest difference in this scenario was that no mineral N fertilisers were added to feedstock cultivation. This reduced the soil N_2O emissions, which is in line with IPCC default values for leguminous crops (IPCC, 2006), where direct N_2O emissions are neglected based on results from Rochette and Janzen (2005). In this study, we added the N-fixing ability to the simulated grass crop in the base scenario, and hence this simulation was not validated against data for N-fixing crops, which needs to be considered when interpreting the results. Because of the lower biogas production, this scenario led to lower mitigation potential than the scenario with increased fertilisation. All the scenarios had a negative temperature response, which meant that the reference system had a larger climate impact than the altered system. However, none of the scenarios achieved negative emissions when only considering the altered system. The lowest temperature response for the altered system was for the N-fixation scenario and the highest was for the increased fertilisation intensity scenario. To increase climate efficiency further, use of fossil fuels in field operations and transport could be excluded and CH_4 losses during digestion and storage could be prevented.

Besides providing a renewable alternative to diesel fuel, the grass-based biogas system investigated here could provide other benefits. For example, cultivating fallow land would increase soil fertility for future biomass cultivation, although of course at the risk of losing the build-up of C stock. The grass biomass produced could also serve as fodder back-up in periods with low fodder production, e.g. due to heatwaves, which are expected to become more frequent with increased global temperature (IPCC, 2014).

Process-based models, such as DNDC, can theoretically be applied to many combinations of geography, climate, cropping systems and management practices. However, existing models are based on the current collective scientific understanding of agroecosystem processes and there are still many knowledge gaps that needs to be filled to improve the models. More basic research is therefore essential, e.g. on the processes underlying soil N_2O formation and soil C balance.

5. Conclusions

In this study, biogas production from grass was assessed using LCA methodology in combination with a process-based agroecosystem model fed with regional-specific data spatially organised with GIS programming. This combined method could be used to design biomass production schemes in other regions, thereby serving as a strategic tool to assist land use planning of local energy production from arable land. The agro-ecosystem models are, however, limited by scientific understanding of the described processes.

The biogas produced from grass grown on fallow reduced the climate impact significantly, by 79–102%, compared with diesel fuel. Variations in soil N_2O emissions between fields explained most of the spatial variation in climate impact in the study region. By implementing the proposed system, the region's biogas production could on average be doubled, which would reduce the climate impact by 9950 Mg CO_2-eq every year and increase soil fertility in the region through increased soil C stock.

Manufacturing of mineral N fertiliser represented approximately one-third of total primary energy input to the altered system and soil N_2O emissions related to N fertilisation were the greatest source of emissions from the grass cultivation system. Excluding N fertiliser by using feedstock crops relying on symbiotic N fixation, such as clover, increased the energy efficiency and resulted in the highest climate mitigation per energy produce biogas (MJ). However, this scenario reduced biogas production, due to the assumption of lower yields. In contrast, increasing the fertilisation rate in grass cultivation entailed a lower mitigation potential per MJ but higher biogas production, which resulted in the highest climate change mitigation potential in the region.

CRediT authorship contribution statement

Johan Nilsson: Conceptualization, Methodology, Software, Formal analysis, Writing - original draft. **Cecilia Sundberg:** Conceptualization, Writing - review & editing. **Pernilla Tidåker:** Conceptualization, Writing - review & editing, Supervision. **Per-Anders Hansson:** Conceptualization, Writing - review & editing, Supervision, Resources, Funding acquisition.

Declaration of competing interest

The authors declare that they have no known competing financial interests or personal relationships that could have appeared to influence the work reported in this paper.

Acknowledgements

This research did not receive any specific grant from funding agencies in the public, commercial or not-for-profit sectors. The authors gratefully acknowledge the contribution of Dana Ghrabeti in providing essential assistance with programming. We also want to thank Brian Grant and Ward Smith (Ottawa Research and Development Centre, Agriculture and Agri-Food Canada) for assistance and valuable discussions regarding the DNDC model.

Appendix A. Supplementary data

Supplementary data to this article can be found online at https://doi.org/10.1016/j.jclepro.2020.122778.

References

Bentrup, F., Hoxha, A., Christensen, B., 2016. Carbon footprint analysis of mineral fertilizer production in Europe and other world regions. In: Proceedings of LCA Food, Dublin, Ireland, 2016 (Dublin, Ireland).

Berglund, M., Börjesson, P., 2006. Assessment of energy performance in the life-cycle of biogas production. Biomass Bioenergy 30, 254–266. https://doi.org/10.1016/j.biombioe.2005.11.011.

Bolinder, M.A., Kätterer, T., Andrén, O., Ericson, L., Parent, L.-E., Kirchmann, H., 2010. Long-term soil organic carbon and nitrogen dynamics in forage-based crop rotations in Northern Sweden (63–64°N). Agric. Ecosyst. Environ. 138, 335–342. https://doi.org/10.1016/j.agee.2010.06.009.

Börjesson, P., Lantz, M., Andersson, J., Björnsson, L., Möller Fredriksson, B., Fröberg, M., Hanarp, P., Hulteberg, C.P., Iverfeldt, E., Lundgren, J., Röj, A., Svensson, H., Zinn, E., 2016. Methane as vehicle fuel – a well to wheel analysis (METDRIV). The Swedish knowledge centre for renewable transportation fuels.

Carlsson, G., Mårtensson, L.-M., Prade, T., Svensson, S.-E., Jensen, E.S., 2017a. Perennial species mixtures for multifunctional production of biomass on marginal land. GCB Bioenergy 9, 191–201. https://doi.org/10.1111/gcbb.12373.

Djomo, S.N., Kasmioui, O.E., Ceulemans, R., 2011. Energy and greenhouse gas balance of bioenergy production from poplar and willow: a review. GCB Bioenergy

3, 181–197. https://doi.org/10.1111/j.1757-1707.2010.01073.x.

Gilhespy, S.L., Anthony, S., Cardenas, L., Chadwick, D., del Prado, A., Li, C., Misselbrook, T., Rees, R.M., Salas, W., Sanz-Cobena, A., Smith, P., Tilston, E.L., Topp, C.F.E., Vetter, S., Yeluripati, J.B., 2014. First 20 years of DNDC (DeNitrification DeComposition): model evolution. Ecol. Model. 292, 51–62. https://doi.org/10.1016/j.ecolmodel.2014.09.004.

Goglio, P., Grant, B.B., Smith, W.N., Desjardins, R.L., Worth, D.E., Zentner, R., Malhi, S.S., 2014. Impact of management strategies on the global warming potential at the cropping system level. Sci. Total Environ. 490, 921–933. https://doi.org/10.1016/j.scitotenv.2014.05.070.

Goglio, P., Smith, W.N., Grant, B.B., Desjardins, R.L., Gao, X., Hanis, K., Tenuta, M., Campbell, C.A., McConkey, B.G., Nemecek, T., Burgess, P.J., Williams, A.G., 2018a. A comparison of methods to quantify greenhouse gas emissions of cropping systems in LCA. J. Clean. Prod. 172, 4010–4017. https://doi.org/10.1016/j.jclepro.2017.03.133.

Goglio, P., Smith, W.N., Worth, D.E., Grant, B.B., Desjardins, R.L., Chen, W., Tenuta, M., McConkey, B.G., Williams, A., Burgess, P., 2018b. Development of Crop.LCA, an adaptable screening life cycle assessment tool for agricultural systems: a Canadian scenario assessment. J. Clean. Prod. 172, 3770–3780. https://doi.org/10.1016/j.jclepro.2017.06.175.

Government Offices of Sweden, 2016. Överenskommelse om den svenska energipolitiken. Government Offices of Sweden. https://www.regeringen.se/artiklar/2016/06/overenskommelse-om-den-svenska-energipolitiken/.

Grant, B.B., Smith, W.N., Campbell, C.A., Desjardins, R.L., Lemke, R.L., Kröbel, R., McConkey, B.G., Smith, E.G., Lafond, G.P., 2016. Comparison of DayCent and DNDC models: case studies using data from long-term experiments on the Canadian prairies. In: Synthesis and Modeling of Greenhouse Gas Emissions and Carbon Storage in Agricultural and Forest Systems to Guide Mitigation and Adaptation. Advances in Agricultural Systems Modeling, vol. 6. https://doi.org/10.2134/advagricsystmodel6.2013.0035.

Hammar, T., Hansson, P.-A., Sundberg, C., 2017. Climate impact assessment of willow energy from a landscape perspective: a Swedish case study. GCB Bioenergy 9, 973–985. https://doi.org/10.1111/gcbb.12399.

Hijazi, O., Munro, S., Zerhusen, B., Effenberger, M., 2016. Review of life cycle assessment for biogas production in Europe. Renew. Sustain. Energy Rev. 54, 1291–1300. https://doi.org/10.1016/j.rser.2015.10.013.

IPCC, 2014. In: Pachauri, R.K., Meyer, L.A. (Eds.), Climate Change 2014: Synthesis Report. Contribution of Working Groups I, II and III to the Fifth Assessment Report of the Intergovernmental Panel on Climate Change [Core Writing Team. IPCC, Geneva Switzerland.

Kätterer, T., Bolinder, M.A., Berglund, K., Kirchmann, H., 2012. Strategies for carbon sequestration in agricultural soils in northern Europe. Acta Agric. Scand. Sect. A Anim. Sci. 62, 181–198. https://doi.org/10.1080/09064702.2013.779316.

Kendall, A., 2012. Time-adjusted global warming potentials for LCA and carbon footprints. Int. J. Life Cycle Assess. 17, 1042–1049. https://doi.org/10.1007/s11367-012-0436-5.

Lewandowski, I., 2015. Securing a sustainable biomass supply in a growing bioeconomy. Glob. Food Secur. 6, 34–42. https://doi.org/10.1016/j.gfs.2015.10.001.

Li, C., Frolking, S., Frolking, T.A., 1992. A model of nitrous oxide evolution from soil driven by rainfall events: 1. Model structure and sensitivity. J. Geophys. Res. Atmospheres 97, 9759–9776. https://doi.org/10.1029/92JD00509.

McMillan, A.M.S., Pal, P., Phillips, R.L., Palmada, T., Berben, P.H., Jha, N., Saggar, S., Luo, J., 2016. Can pH amendments in grazed pastures help reduce N2O emissions from denitrification? – the effects of liming and urine addition on the completion of denitrification in fluvial and volcanic soils. Soil Biol. Biochem. 93, 90–104. https://doi.org/10.1016/j.soilbio.2015.10.013.

Miller, S.A., Landis, A.E., Theis, T.L., 2006. Use of Monte Carlo analysis to characterize nitrogen fluxes in agroecosystems. Environ. Sci. Technol. 40, 2324–2332. https://doi.org/10.1021/es0518878.

Myhre, G., Bréon, F.-M., Collins, W., Fuglestvedt, J., Huang, J., Koch, D., Lamarque, J.-F., Lee, D., Mendoza, B., Nakajima, T., Robock, A., Stephens, G., Takemura, T., Zhang, H., 2013a. Anthropogenic and natural radiative forcing. In: Stocker, T.F., Qin, D., Plattner, G.-K., Tignor, M., Allen, S.K., Boschung, J., Nauels, A., Xia, Y., Bex, V., Midgley, P.M. (Eds.), Climate Change 2013: the Physical Science Basis. Contribution of Working Group I to the Fifth Assessment Report of the Intergovernmental Panel on Climate Change. Cambridge University Press, Cambridge, United Kingdom and New York, NY, USA.

Nilsson, J., Tidåker, P., Sundberg, C., Henryson, K., Grant, B., Smith, W., Hansson, P.-A., (Unpublished results). Assessing the Climate Impact and Eutrophication of Grass Cultivation at Five Sites in Sweden. (Submitted).

Nitschelm, L., Aubin, J., Corson, M.S., Viaud, V., Walter, C., 2016. Spatial differentiation in Life Cycle Assessment LCA applied to an agricultural territory: current practices and method development. J. Clean. Prod. 112, 2472–2484. https://doi.org/10.1016/j.jclepro.2015.09.138.

Poeplau, C., Kätterer, T., Bolinder, M.A., Börjesson, G., Berti, A., Lugato, E., 2015. Low stabilization of aboveground crop residue carbon in sandy soils of Swedish long-term experiments. Geoderma 237–238, 246–255. https://doi.org/10.1016/j.geoderma.2014.09.010.

Russenes, A.L., Korsaeth, A., Bakken, L.R., Dörsch, P., 2016. Spatial variation in soil pH controls off-season N2O emission in an agricultural soil. Soil Biol. Biochem. 99, 36–46. https://doi.org/10.1016/j.soilbio.2016.04.019.

Saxton, K.E., Rawls, W.J., 2006. Soil water characteristic estimates by texture and organic matter for hydrologic solutions. Soil Sci. Soc. Am. J. 70, 1569–1578. https://doi.org/10.2136/sssaj2005.0117.

SCB, 2017. Set-aside (Fallow) 2016 divided by short and long term set-aside. https://www.scb.se/en/finding-statistics/statistics-by-subject-area/environment/fertilisers-and-lime/use-of-fertilisers-and-animal-manure-and-cultivation-measures-in-agriculture/pong/tables-and-graphs/cultivation-measures/set-aside-fallow-2016-divided-by-short-and-long-term-set-aside/.

SCB, 2018a. Use of Agricultural Land 2018. Final Statistics. JO10 SM 1802. Statistics Sweden.

SCB, 2018b. Production of cereals, dried pulses, oilseed crops, potatoes, and temporary grasses in 2017. In: Final Statistics. JO 16 SM 1801. Statistics Sweden.

SEA, 2019. Drivmedel 2018. Swedish Energy Agency.

SOU, 2013. Fossilfrihet På Väg – Del 1 (SOU 2013:84). Statens Offentliga Utredningar. Government Offices of Sweden.

Styles, D., Dominguez, E.M., Chadwick, D., 2016a. Environmental balance of the UK biogas sector: an evaluation by consequential life cycle assessment. Sci. Total Environ. 560–561, 241–253. https://doi.org/10.1016/j.scitotenv.2016.03.236.

Tatzber, M., Stemmer, M., Spiegel, H., Katzlberger, C., Landstetter, C., Haberhauer, G., Gerzabek, M.H., 2012. 14C-labeled organic amendments: characterization in different particle size fractions and humic acids in a long-term field experiment. Geoderma 177–178, 39–48. https://doi.org/10.1016/j.geoderma.2012.01.028.

Tidåker, P., Bergkvist, G., Bolinder, M., Eckersten, H., Johnsson, H., Kätterer, T., Weih, M., 2016a. Estimating the environmental footprint of barley with improved nitrogen uptake efficiency—a Swedish scenario study. Eur. J. Agron. 80, 45–54. https://doi.org/10.1016/j.eja.2016.06.013.

Tidåker, P., Rosenqvist, H., Bergkvist, G., 2016b. Räkna med vall - hur påverkas ekonomi och miljö när vall införs i spannmålsdominerade växtföljder?. In: Rapport 445, JTI – Institutet För Jordbruks- Och Miljöteknik. Uppsala, Sweden.

Tilman, D., Socolow, R., Foley, J.A., Hill, J., Larson, E., Lynd, L., Pacala, S., Reilly, J., Searchinger, T., Somerville, C., Williams, R., 2009. Beneficial biofuels—the food, energy, and environment trilemma. Science 325, 270–271. https://doi.org/10.1126/science.1177970.

Uppsala Vatten, 2017a. Miljörapport 2017 - Biogasanläggningen Vid Kungsängens Gård. Uppsala Vatten.

Weiland, P., 2010. Biogas production: current state and perspectives. Appl. Microbiol. Biotechnol. 85, 849–860. https://doi.org/10.1007/s00253-009-2246-7.